PHYSICAL REVIEW D **93,** 085030 (2016)

Perturbative thermodynamics at nonzero isospin density for cold QCD

Thorben Graf and Juergen Schaffner-Bielich
Institute for Theoretical Physics, Goethe University,
Max-von-Laue-Straße 1, D–60438 Frankfurt am Main, Germany

Eduardo S. Fraga
Instituto de Fisica, Universidade Federal do Rio de Janeiro,
Caixa Postal 68528 Rio de Janeiro, RJ 21941-972, Brazil
(Received 17 December 2015; published 21 April 2016)

We use next-to-leading order in perturbation theory to investigate the effects of a finite isospin density on the thermodynamics of cold strongly interacting matter. Our results include nonzero quark masses and are compared to lattice data.

DOI: 10.1103/PhysRevD.93.085030

I. INTRODUCTION

The thermodynamics of strongly interacting matter at nonvanishing isospin chemical potential, μ_I, is relevant in different realms of physics since there are several systems where the amounts of protons and neutrons are not the same. In the formation process of neutron stars, the initial proton fraction in supernovae is ~ 0.4, which reduces with time to values of less than 0.1 in cold neutron stars [1,2]. In the early universe, shortly after the big bang, a large asymmetry in the lepton sector that could shift the equilibrium conditions at the cosmological quark-hadron transition is allowed [3]. And, of course, in high-energy heavy-ion collisions, the proton-to-neutron ratio is $\sim 2/3$ in Au or Pb beams.

The phase diagram of QCD at finite temperature and isospin density is rich in phenomenology and has been investigated for more than a decade [4,5]. During this time, several studies have been performed within effective models on the lattice and, most recently, even perturbatively [6–25]. Although Monte Carlo simulations do not suffer from the sign problem since the fermion determinant remains real at nonzero μ_I, lattice calculations at nonzero isospin have been performed so far with unphysical quark masses [7,8,10,11,13,14,24], which still limits their quantitative predictive power.

In this paper, we use next-to-leading order in perturbation theory to investigate the effects of a finite isospin density on the thermodynamics of cold ($T=0$) strongly interacting matter which includes nonzero quark masses. Whenever possible, our results are compared to lattice data from Ref. [26]. The paper is organized as follows: Sec. II presents a brief discussion of the physical scenario and our setup, Sec. III shows and discusses our results for the thermodynamical quantities computed, and Sec. IV contains our final remarks.

II. PHYSICAL SCENARIO AND SETUP

The phase diagram of QCD in the temperature versus isospin chemical potential plane is illustrated in Fig. 1, which should be seen as a cartoon. Along the temperature axis ($\mu_I = 0$), there is no phase transition, according to lattice calculations at physical quark masses [27]. At high isospin density, for values of μ_I above the pion mass m_π, pion condensation takes place for not too large temperatures. At very high isospin density, a Fermi liquid with Cooper pairing is formed as a consequence of an attractive interaction between quarks in the isospin channel [4]. In contrast to the temperature versus baryon chemical potential (μ_B) plane, there is a first-order deconfinement phase transition for large μ_I within the condensed phase, as indicated by the green line in Fig. 1. The authors of Ref. [5] conjecture that the phase transition line ends at a second-order point.[1] According to Ref. [14], the chiral phase transition is located along the purple line in Fig. 1.

Lattice calculations of Ref. [26] were run at nonzero μ_I and at a fixed temperature of $T = 20$ MeV. The values of μ_I covered in the simulations are indicated by the horizontal red line in Fig. 1. Our perturbative calculations were performed for values of the isospin chemical potential which are represented by the blue solid line, at $T = 0$. This difference should not be significant given the comparatively large values of μ_I, as was verified *a posteriori*.

The energy scale of the (de)confinement transition was computed in Ref. [28] using an effective model description and found to be quite low, $\Lambda_{\rm Con} \approx 15$–$50$ MeV. Numerical values for the (de)confinement scale were also computed in Refs. [7,13,14].

The phenomenon of pairing mentioned above should not be relevant for our perturbative study, in the same fashion that happens at nonzero (large) baryon chemical potential. The gap Δ is exponentially suppressed for small values of g, in the domain of validity of perturbation theory [4,29],

$$\Delta = b|\mu_I| g^{-5} e^{-c/g}, \tag{1}$$

[1]Other investigations suggest different scenarios concerning the existence of this critical point [28].

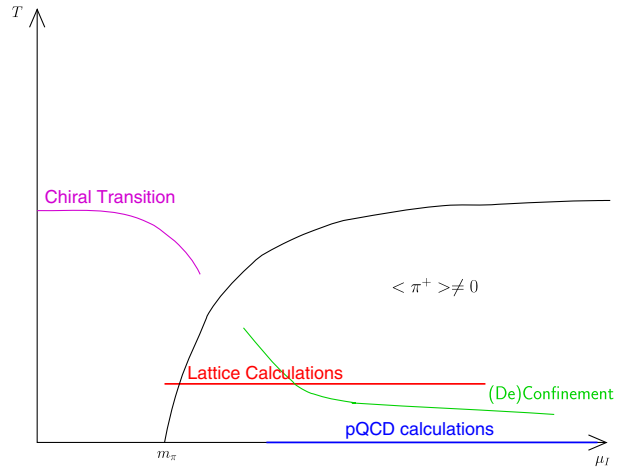

FIG. 1. Cartoon of the phase diagram of QCD at finite temperature and isospin chemical potential based on results from Refs. [14,28].

where $c = 3\pi^2/2$ and $g = g(|\mu_I|)$ is the running coupling. We expect that the corresponding gap for nonzero isospin chemical potential will stay below $\Delta \sim 300$–400 MeV and, hence, will give a subleading contribution to the thermodynamic potential $\sim\mu_I^2\Delta^2$ [30].

Since the lattice calculations (red line in Fig. 1) might cross the deconfinement transition (green line) as conjectured in Ref. [28], one can expect that perturbative calculations could provide a reasonable description of lattice results for large enough values of μ_I. With the help of Fig. 2 in Ref. [28], a quantitative statement about the scale of μ_I at which the deconfined phase appears can be made: for $\mu_I \simeq 4$ GeV, the deconfinement phase transition line crosses $T = 20$ MeV, the value used in the lattice simulations of Ref. [26] to which we compare our findings.

For $T = 0$, the expressions for the thermodynamic potential are available in analytic form up to $\mathcal{O}(\alpha_s^2)$. The one massive flavor contribution (leading and next-to-leading order) in the $\overline{\text{MS}}$ scheme is given by (see, e.g., Refs. [31–33])

$$\Omega^{(0)} = -\frac{N_C}{12\pi^2}\left[\mu u\left(\mu^2 - \frac{5}{2}m^2\right) + \frac{3}{2}m^4\ln\left(\frac{\mu+u}{m}\right)\right], \tag{2}$$

$$\Omega^{(1)} = \frac{\alpha_s N_G}{16\pi^3}\left\{3\left[m^2\ln\left(\frac{\mu+u}{m}\right) - \mu u\right]^2 - 2u^4 + m^2\left[6\ln\left(\frac{\Lambda}{m}\right) + 4\right]\left[\mu u - m^2\ln\left(\frac{\mu+u}{m}\right)\right]\right\}, \tag{3}$$

where $u \equiv \sqrt{\mu^2 - m^2}$ and N_C and N_G are the numbers of colors and gluons, respectively. For calculations with $2+1$ massive quark flavors, we introduce the isospin chemical potential in the following way:

$$\begin{aligned} &\mu_I = \mu_u - \mu_d, \qquad \mu_q = \frac{\mu_u + \mu_d}{2}, \\ &\mu_u = \mu_q + \frac{1}{2}\mu_I, \qquad \mu_d = \mu_q - \frac{1}{2}\mu_I, \\ &\mu_s = 0, \end{aligned} \tag{4}$$

where μ_q is the quark chemical potential. We assume $\mu_q = 0$ in what follows.

III. RESULTS

In order to compare our results with those from lattice simulations presented in Ref. [26], we adjust our parameters accordingly. The strange quark chemical potential μ_s is chosen to be zero, and the vacuum pion mass is taken to be $m_\pi = 390$ MeV. This corresponds to light quark masses $m_{u/d}$ and a strange quark mass m_s given by

$$m_{u/d} = 35 \text{ MeV} \quad \text{and} \quad m_s = 875 \text{ MeV}, \tag{5}$$

as extracted from the GOR relation [34]. Since $\mu_s = 0$, the strange quark plays no role in our analysis.

Our calculations implement a running coupling α_s [35,36],

$$\alpha_s(\Lambda) = \frac{4\pi}{\beta_0 L}\left[1 - 2\frac{\beta_1}{\beta_0^2}\frac{\ln L}{L}\right], \tag{6}$$

where $L = 2\ln(\Lambda/\Lambda_{\overline{\text{MS}}})$, $\beta_0 = 11 - 2N_f/3$ and $\beta_1 = 51 - 19N_f/3$. The scale $\Lambda_{\overline{\text{MS}}}$ is fixed by requiring $\alpha_s \simeq 0.3$ at $\Lambda = 2$ GeV [36], and one obtains $\Lambda_{\overline{\text{MS}}} \simeq 380$ MeV. See also Ref. [31] for details. With these conventions, the only freedom left is the choice of the renormalization scale Λ, which is set to $\Lambda = 2\mu_I$ in all of our numerical simulations.

From the thermodynamic potential, Eqs. (2) and (3), we have full access to all thermodynamical quantities, such as the pressure,

$$\Omega = -pV, \tag{7}$$

the isospin density ρ_I,

$$\rho_I = \frac{\partial p}{\partial \mu_I}, \tag{8}$$

and the energy density ε (for $T = 0$),

$$\varepsilon = \frac{\partial p}{\partial \mu_I}\mu_I - p. \tag{9}$$

In Figs. 2 and 3, we compare our results with lattice data from Ref. [26]. In Fig. 2, the ratio of energy density to

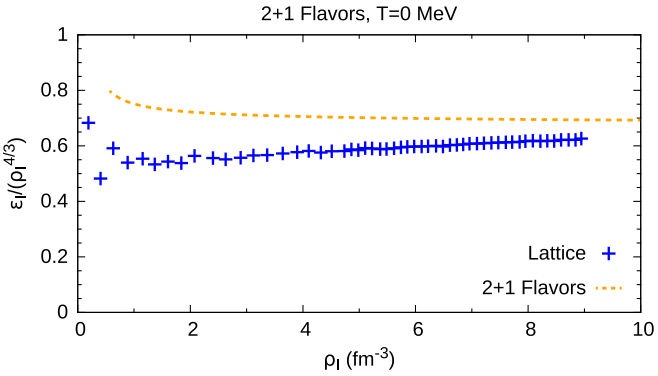

FIG. 2. Comparison of the ratio of energy density to (isospin density)$^{4/3}$ versus the isospin density with lattice results from Ref. [26].

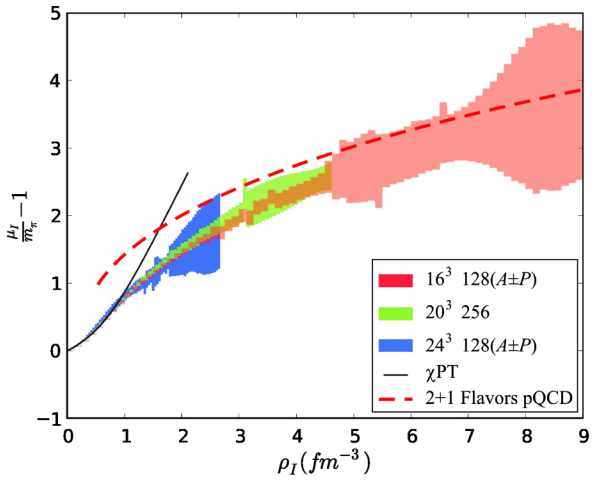

FIG. 3. Comparison of the isospin chemical potential versus the isospin density with lattice results from Ref. [26].

(isospin density)$^{4/3}$ is plotted against the isospin density. One can see that, for increasing isospin density, the two curves approach each other, as expected from asymptotic freedom, although perturbation theory systematically overestimates this quantity within the range of available lattice data extracted from Ref. [26]. We stress that the density dependence with a power of 4/3 is characteristic for an ultrarelativistic Fermi gas, the asymptotic limit at high chemical potentials. Note that an isospin density of roughly 9 fm^{-3} corresponds to a value of $\mu_I = 2$ GeV. In Fig. 3, the isospin chemical potential (subtracted by and normalized by the pion mass) is displayed versus the isospin density. The results from pQCD agree well with those that correspond to a band of lattice results extracted from Ref. [26] for values of the isospin chemical potential larger than about a few times the pion mass.

In Fig. 4, we exhibit the energy density normalized by the Stefan-Boltzmann (SB) form versus μ_I/m_π and also compare with the corresponding band of lattice data

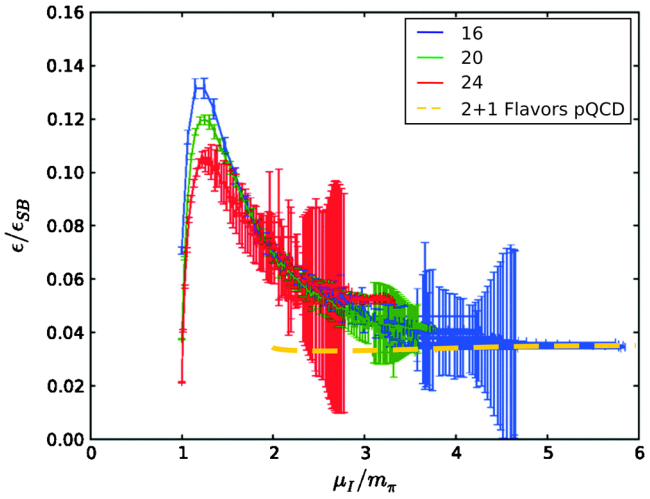

FIG. 4. Energy density normalized by the isospin-related Stefan-Boltzmann (SB) form versus μ_I/m_π. Lattice results from Ref. [26].

extracted from Ref. [26] which defines the SB limit via the isospin chemical potential as

$$\varepsilon_{\mathrm{SB}} = \frac{N_f N_c}{4\pi^2}\mu_I^4. \tag{10}$$

In terms of quark degrees of freedom, the SB limit is given as a function of the quark chemical potential,

$$\varepsilon_{\mathrm{SB}} = \frac{N_f N_c}{4\pi^2}\mu^4 = \frac{N_f N_c}{4\pi^2}\frac{\mu_I^4}{16}, \tag{11}$$

which gives, via the relation $\mu = \frac{1}{2}\mu_I$, a factor of 16 difference in the corresponding SB limits. The latter one would be the limit for a gas of quarks at zero temperature and high chemical potentials and, hence, also the SB limit for pQCD calculations.

One sees in Fig. 4 that, for $\mu_I > 2m_\pi$, the pQCD results are compatible with the ones from the lattice. The peak at $\mu_I \approx m_\pi$ cannot be reproduced since it is caused by the pion condensate which is not captured by perturbation theory. Simulations that are based on chiral perturbation theory (χPT) are indeed able to calculate this maximum [37]. By maximizing the static chiral Lagrangian density, the authors derive an analytic expression for the normalized energy density at the peak at leading order. In general, lattice data are well reproduced by χPT at leading order for low densities, $\mu_I < 2m_\pi$. However, for $\mu_I > 2m_\pi$ the results of chiral perturbation theory asymptotically approach zero as only pion degrees of freedom are incorporated. This is in contrast to the lattice data which reach, at asymptotically high isospin chemical potentials, our results from pQCD which are based on quark degrees of freedom. In Fig. 5, the same data as Fig. 4 are shown with regard to the SB limit for a gas of quarks, i.e., rescaled by a factor of 16 which

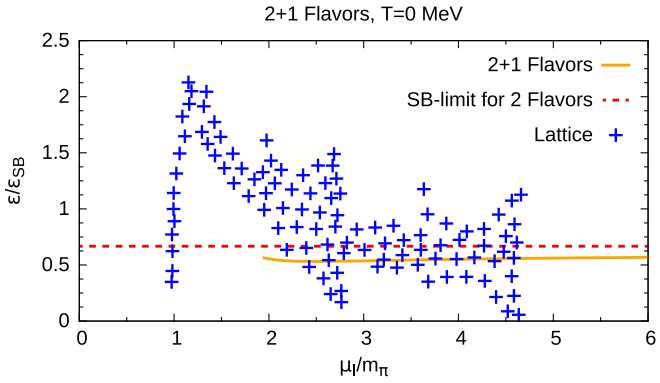

FIG. 5. Rescaled energy density by an isospin-related factor of 16 (see text for details) versus μ_I/m_π. The pQCD results approach the SB limit related to the quark chemical potential for two flavors as the strange quark is not appearing in the calculation.

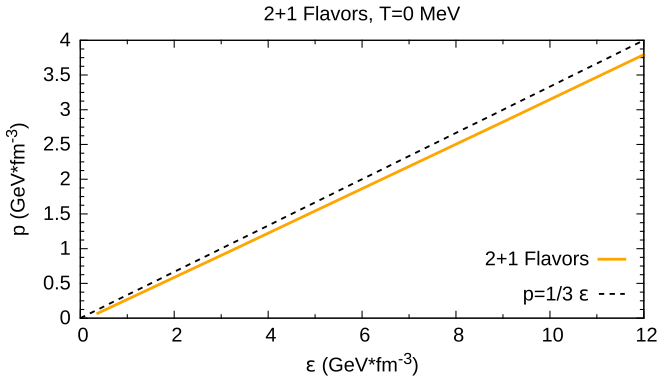

FIG. 6. Equation of state compared to the ideal case.

appears when $\mu = \frac{1}{2}\mu_I$. The SB limit for two flavors (horizontal line) is also sketched in Fig. 5 because the strange quark is not contributing in our calculations as $\mu_s = 0$ so that this SB limit should be considered as the actual limit of a free gas of quarks and gluons. In this sense, our results (orange line) are obviously very close to this limit, which is consistent with the notion of asymptotic freedom.

Finally, in Fig. 6, we plot the equation of state to exhibit the deviations from ideality, i.e., $\varepsilon = 3p$. The equation of state follows closely the one for an ideal ultrarelativistic gas.

IV. SUMMARY

We investigated thermodynamic properties of massive cold quark matter at zero temperature and baryon chemical potential and nonvanishing isospin density at next-to-leading order in perturbation theory, and compared our results with recent lattice data.

The ratio of energy density to (isospin density)$^{4/3}$ versus isospin density shows that lattice data and our pQCD results get closer for high densities. Both seem to follow a $\rho_I^{4/3}$ scaling at high densities, which agrees with the limit for an ultrarelativistic degenerate Fermi gas. The isospin chemical potential plotted against the isospin density shows that the pQCD results and lattice results converge for values of $\mu_I \gtrsim 3m_\pi$. This is also true for the comparison of the normalized energy density as a function of the isospin chemical potential. The normalized energy density is essentially constant in the high-density limit, as expected.

We also verified that the energy density from the pQCD calculation is not too far from the Stefan-Boltzmann limit for two flavors since the strange quark does not appear in the dense medium under consideration. Furthermore, the deviations from an ideal equation of state are small.

In summary, the results from pQCD already seem to be close to the lattice data for values of $\mu_I \gtrsim 3m_\pi$, even in the region of pion condensate. It seems that the effect from the gap is suppressed for small values of the coupling constant, as anticipated, and gives a small contribution to the thermodynamic potential which is then dictated at high chemical potentials by a nearly free gas of quarks.

ACKNOWLEDGMENTS

The authors want to thank Rainer Stiele, Lorenz von Smekal, Nils Strodthoff and William Detmold for fruitful discussions. E. S. F. is grateful for the kind hospitality of the ITP group at Frankfurt University, where this work was initiated. T. G. is supported by the Helmholtz International Center for FAIR and the Helmholtz Graduate School HGS-HIRe. The work of E. S. F. is partially supported by CAPES, CNPq and FAPERJ.

[1] M. Prakash, J. M. Lattimer, J. A. Pons, A. W. Steiner, and S. Reddy, Lect. Notes Phys. **578**, 364 (2001).
[2] F. Weber, Prog. Part. Nucl. Phys. **54**, 193 (2005).
[3] D. J. Schwarz and M. Stuke, J. Cosmol. Astropart. Phys. 11 (2009) 025; 10 (2010) E01.
[4] D. Son and M. A. Stephanov, Phys. Rev. Lett. **86**, 592 (2001).
[5] D. Son and M. A. Stephanov, Phys. At. Nucl. **64**, 834 (2001).
[6] D. Toublan and J. B. Kogut, Phys. Lett. B **564**, 212 (2003).

[7] J. B. Kogut and D. K. Sinclair, Phys. Rev. D **70**, 094501 (2004).
[8] J. B. Kogut and D. K. Sinclair, Nucl. Phys. B, Proc. Suppl. **140**, 526 (2005).
[9] D. Toublan and J. B. Kogut, Phys. Lett. B **605**, 129 (2005).
[10] J. B. Kogut and D. K. Sinclair, in arXiv:hep-lat/0504003.
[11] D. K. Sinclair and J. B. Kogut, Proceedings, 24th International Symposium on Lattice Field Theory (Lattice 2006), in *Proc. Sci.*, LAT2006 (2006) 147 [arXiv:hep-lat/0609041].
[12] J. O. Andersen, Phys. Rev. D **75**, 065011 (2007).
[13] P. de Forcrand, M. A. Stephanov, and U. Wenger, Proceedings, 25th International Symposium on Lattice field theory (Lattice 2007), in *Proc. Sci.*, LAT2007 (2007) 237 [arXiv:0711.0023].
[14] P. Cea, L. Cosmai, M. D'Elia, A. Papa, and F. Sanfilippo, Phys. Rev. D **85**, 094512 (2012).
[15] E. Fraga, L. Palhares, and C. Villavicencio, Phys. Rev. D **79**, 014021 (2009).
[16] L. Palhares, E. Fraga, and C. Villavicencio, Nucl. Phys. **A820**, 287C (2009).
[17] J. O. Andersen and L. Kyllingstad, J. Phys. G **37**, 015003 (2010).
[18] K. Kamikado, N. Strodthoff, L. von Smekal, and J. Wambach, Phys. Lett. B **718**, 1044 (2013).
[19] T. Sasaki, Y. Sakai, H. Kouno, and M. Yahiro, Phys. Rev. D **82**, 116004 (2010).
[20] H. Ueda, T. Z. Nakano, A. Ohnishi, M. Ruggieri, and K. Sumiyoshi, Phys. Rev. D **88**, 074006 (2013).
[21] R. Stiele, E. S. Fraga, and J. Schaffner-Bielich, Phys. Lett. B **729**, 72 (2014).
[22] T. Xia, L. He, and P. Zhuang, Phys. Rev. D **88**, 056013 (2013).
[23] T. Kanazawa and T. Wettig, J. High Energy Phys. 10 (2014) 55.
[24] G. Endrodi, Phys. Rev. D **90**, 094501 (2014).
[25] J. O. Andersen, N. Haque, M. G. Mustafa, and M. Strickland, arXiv:1511.04660.
[26] W. Detmold, K. Orginos, and Z. Shi, Phys. Rev. D **86**, 054507 (2012).
[27] Y. Aoki, G. Endrodi, Z. Fodor, S. D. Katz, and K. K. Szabo, Nature **443**, 675 (2006).
[28] T. D. Cohen and S. Sen, Nucl. Phys. **A942**, 39 (2015).
[29] D. T. Son, Phys. Rev. D **59**, 094019 (1999).
[30] M. Alford and K. Rajagopal, J. High Energy Phys. 06 (2002) 031.
[31] E. S. Fraga and P. Romatschke, Phys. Rev. D **71**, 105014 (2005).
[32] A. Kurkela, P. Romatschke, and A. Vuorinen, Phys. Rev. D **81**, 105021 (2010).
[33] T. Graf, J. Schaffner-Bielich, and E. S. Fraga, arXiv:1507.08941.
[34] M. Gell-Mann, R. Oakes, and B. Renner, Phys. Rev. **175**, 2195 (1968).
[35] J. Vermaseren, S. Larin, and T. van Ritbergen, Phys. Lett. B **405**, 327 (1997).
[36] S. Eidelman *et al.* (Particle Data Group), Phys. Lett. B **592**, 1 (2004).
[37] S. Carignano, A. Mammarella, and M. Mannarelli, arXiv: 1602.01317.